Simultaneous intravascular large B-cell lymphoma and papillary thyroid carcinoma: A case report

JINXIANG LIANG[1,2], JIE LI[2], BINGJIE LI[3], JIE YANG[2], QIANG WEI[4] and YAN LI[2]

[1]Department of Graduate School, Hebei North University, Zhangjiakou, Hebei 075031, P.R. China; [2]Department of Haematology, Hebei General Hospital, Shijiazhuang, Hebei 050051, P.R. China; [3]Department of Pathology, Hebei General Hospital, Shijiazhuang, Hebei 050000, P.R. China; [4]Department of Nuclear Medicine, Hebei General Hospital, Shijiazhuang, Hebei 050000, P.R. China

Received October 24, 2024; Accepted February 4, 2025

DOI: 10.3892/mco.2025.2833

Abstract. Intravascular large B-cell lymphoma (IVLBCL) is a rare subtype of B-cell lymphoma. The concurrence of IVLBCL and papillary thyroid carcinoma (PTC) is extremely rare. A 63-year-old woman was diagnosed with double-expression IVLBCL that presented as a hemophagocytic syndrome, complicated by PTC. IVLBCL was diagnosed by positron emission tomography/computed tomography (PET/CT) before bone marrow biopsy. Immunofixation electrophoresis displayed M proteins positive and IgG kappa light chains that the differential diagnosis should have included both multiple myeloma and IVLBCL. After treatment with rituximab, cyclophosphamide, hydroxydaunorubicin, vincristine, prednisone and etoposide, the patient's cytokine titres and other laboratory indicators returned to normal. PET/CT showed that complete remission had been achieved. She has been taking zanubrutinib for 1.5 years and remains in remission. This is a report of a patient with hemophagocytic syndrome-associated IVLBCL with *CCND1* and *DNMT3A* gene mutations combined with PTC and describes changes before and after treatment.

Introduction

Intravascular large B-cell lymphoma (IVLBCL), which has an incidence rate of ~0.095/100,000 individuals (1) and accounts for 1% of B-cell lymphomas (2), is characterized by confining within the lumina of small to medium-sized blood vessels, particularly capillaries (3). It can involve all organs, particularly the central nervous system, skin, kidney, lung and adrenal glands, but rarely involves the thyroid (4). The pathological mechanism underlying development of IVLBCL involves B-cell receptor/nuclear factor-κB signaling, which leads to inhibition of apoptosis (5). Hemophagocytic syndrome (HPS)-associated IVLBCL usually portends a poor prognosis and is necessary for diagnosis early. However, IVLBCL presents with numerous non-specific signs and symptoms which makes it difficult to diagnose. Most of the patients were assessed as stage IV at the time of diagnosis and a long-term survival fraction between 20-40% due to the aggressive (6). Rituximab, cyclophosphamide, hydroxydaunorubicin, vincristine, prednisone and high-dose methotrexate plus intrathecal chemotherapy are a safe and active treatment for patients with IVLBCL without apparent central nervous system involvement at diagnosis (7). In the present report, such a case is documented and the possible pathogenesis is explored.

Case presentation

A 63-year-old-woman presented to the Haematology department of Hebei General Hospital (Shijiazhuang, China) in September 2022, with a persistent high fever lasting a month, dry mouth and eyes, and partial tooth loss. A detailed examination showed body temperature 35.7-40˚C, pulse 112/min, respiration 21/min, blood pressure 123/64 mmHg, clear consciousness, small, palpable, red spots in the neck, chest and both lower extremities.

The main laboratory findings are shown in Table I and suggest Epstein-Barr virus (EBV) infection. An ophthalmologist diagnosed xerophthalmia. Bone marrow biopsy samples were positive for CD20 (Fig. 1) and BCL2 and C-myc large cells were identified within vascular spaces, resulting in a diagnosis of double-expression IVLBCL. Immunostaining also revealed that the tumour cells were positive for PAX-5, CD31, CD34, CyclinD1 and Mum1 (Fig. S1), and negative for CD10, BCL6 and CD30; the Ki-67 index was 80%. Flow cytometric analyses of bone marrow revealed positivity for CD20, CD22, CD79b and lambda chains and were negative for CD38, CD138 and kappa (Fig. S2). In addition, positron emission tomography/computed tomography (PET/CT)

Correspondence to: Dr Yan Li, Department of Haematology, Hebei General Hospital, 348 Heping West Road, Xinhua, Shijiazhuang, Hebei 050051, P.R. China
E-mail: yanli0816@hbghospital.cn

Abbreviations: CT, computed tomography; EBV, Epstein-Barr virus; PET/CT, positron emission tomography/computed tomography; HPS, hemophagocytic syndrome; HLH, hemophagocytic lymphohistiocytosis; IVLBCL, intravascular large B-cell lymphoma; MRI, magnetic resonance imaging; PTC, papillary thyroid carcinoma

Key words: cytogenetic, gene mutations, IVLBCL, PTC, diagnosis, treatment

Table I. Laboratory findings.

	Biomarker	Value	Normal range/limit
CRP	CRP	223.7 mg/λ↑	0-10
Complete blood count	White blood cells	$5.12x10^9$/l	3.5-9.5
	Neutrophils	$3.86x10^9$/l	1.8-6.3
	Mononuclear	$0.25x10^9$/l↑	0.1-0.6
	Eosinophils	0↓	0.02-0.52
	Red blood cells	$3.43x10^{12}$/l	3.8-5.1
	Haemoglobin	79 g/l↓	115-150
	Peripheral T cell	$54x10^9$/l↓	125-350
Biochemistry	Lactate dehydrogenase	2,323.5 U/l↑	120-250
Immunoglobulin	Complement C1q	310.9 mg/l↑	159-233
Cytokines	IL-6	309.3 pg/ml↑	≤7
	IL-8	70.4 pg/ml↑	≤62
	IL-10	107.2 pg/ml↑	≤9.1
	IFN-γ	116.5 pg/ml↑	≤13.2
	TNF-α	62.7 pg/ml↑	≤8
EBV PCR	-	$8.09x10^3$↑	0
sCD25, NK cell activity	-	17.634 pg/ml↑	0-6,400
	-	19.12%	≥15.11%
Serum iron β_2 microglobulin	-	1,366 ng/ml	13-150
	-	3.726 μg/ml↑	0.9-2.7
Antinuclear antibodies	-	1:1,000	<1:100

CRP, C-reactive protein.

showed splenomegaly and hypermetabolism, and bilateral lung and bone marrow diffuse hypermetabolism, resulting in a diagnosis of IVLBCL before bone marrow biopsy (Fig. 2). Our patient thus met the five diagnostic criteria for hemophagocytic lympho-histiocytosis (HLH), namely fever, splenomegaly, cytopenia, ferritin ≥500 ng/ml, sCD 25 ≥2,400 U/ml and a bone marrow sample showing hemophagocytes (Fig. 1) (8). Cranial magnetic resonance imaging (MRI) revealed a hyperintense lesion in the central pons (Fig. 3). Thyroid ultrasound indicated hypoechoic thyroid nodules. Papillary thyroid carcinoma (PTC) was diagnosed by fine needle aspiration biopsy (Fig. 1). Immunofixation electrophoresis displayed M proteins positive and IgG kappa light chains (Fig. S3). Next-generation sequencing of bone marrow yielded mutations for the genes of DNMT3A exon13, DNMT3A exon8, FAT1 exon6 and CCND1 exon3. Nucleic acid extraction was performed using the Blood Genomic DNA Extraction Kit (0.1-1 ml; cat. no. YDP348-03; Tiangen Biotech Co., Ltd.). Nucleic acid quality inspection was performed using a NANODROP ONE (Thermo Fisher Scientific, Inc.) to measure the preliminary DNA concentration, A260/280 and A260/230, where A260 is the absorption wavelength of the highest absorption peak of nucleic acid and A280 is the absorption wavelength of the highest absorption peak of protein. A230 is the absorption wavelength of the highest absorption peak of carbohydrates.

A260/280 and A260/230 are indicative values of nucleic acid purity. An A260/280 ratio of 1.8-2.0 and an A260/230 ratio of 2.0-2.2 indicate that the purity of DNA is favourable. Qubit 4.0 fluorometer (cat. no. Q33238; Thermo Fisher Scientific, Inc.) detection was used as the standard for library construction input. Raw samples were analyzed by electrophoresis (2.5% agarose gels) using DNA marker (BM401-01; TransGen Biotech Co., Ltd.) to initially confirm DNA integrity.

The sequencing protocol was paired-end 150 bp sequencing. The DNA library was constructed with a commercial kit (cat. no. 20025524; Illumina DNA Prep with Enrichment). The library quality control was performed using a Qubit 4.0 to detect the library concentration, and Agilent DNF-915 Reagent Kits (Agilent Technologies, Inc.) were used to perform fragment analysis quality control on the Agilent 5200 platform (Agilent Technologies, Inc.). The average fragments ranged between 330 and 390 bp [dilution conversion formula for the concentration of the library: 1.25 nm x average molar mass of bases (660) x average fragment length of library (330-390 bp)/106=0.27-0.32 ng/μl (0.4-0.48 nM)]. Hybridization was performed using the Next era DNA Flex Pre-Enrichment Library Prep and Enrichment Reagents 96 samples, and targeted capture amplification of the target region was performed with probes manufactured by Tianjin Xiehe Bojing Medical Diagnostic Technology Co., Ltd. The sequencing platform was Illumina novaseq6000 (Illumina, Inc.) with the NovaSeq6000 S1 Reagents Kit v1.5 (300 cycles; cat. no. 20028318). The sequencing input protocol was as follows: Samples to be uploaded were prepared and their molar concentrations were calculated, then the libraries were denatured and samples were detected at a concentration of 250 pM(1.25 nM). The molarity was

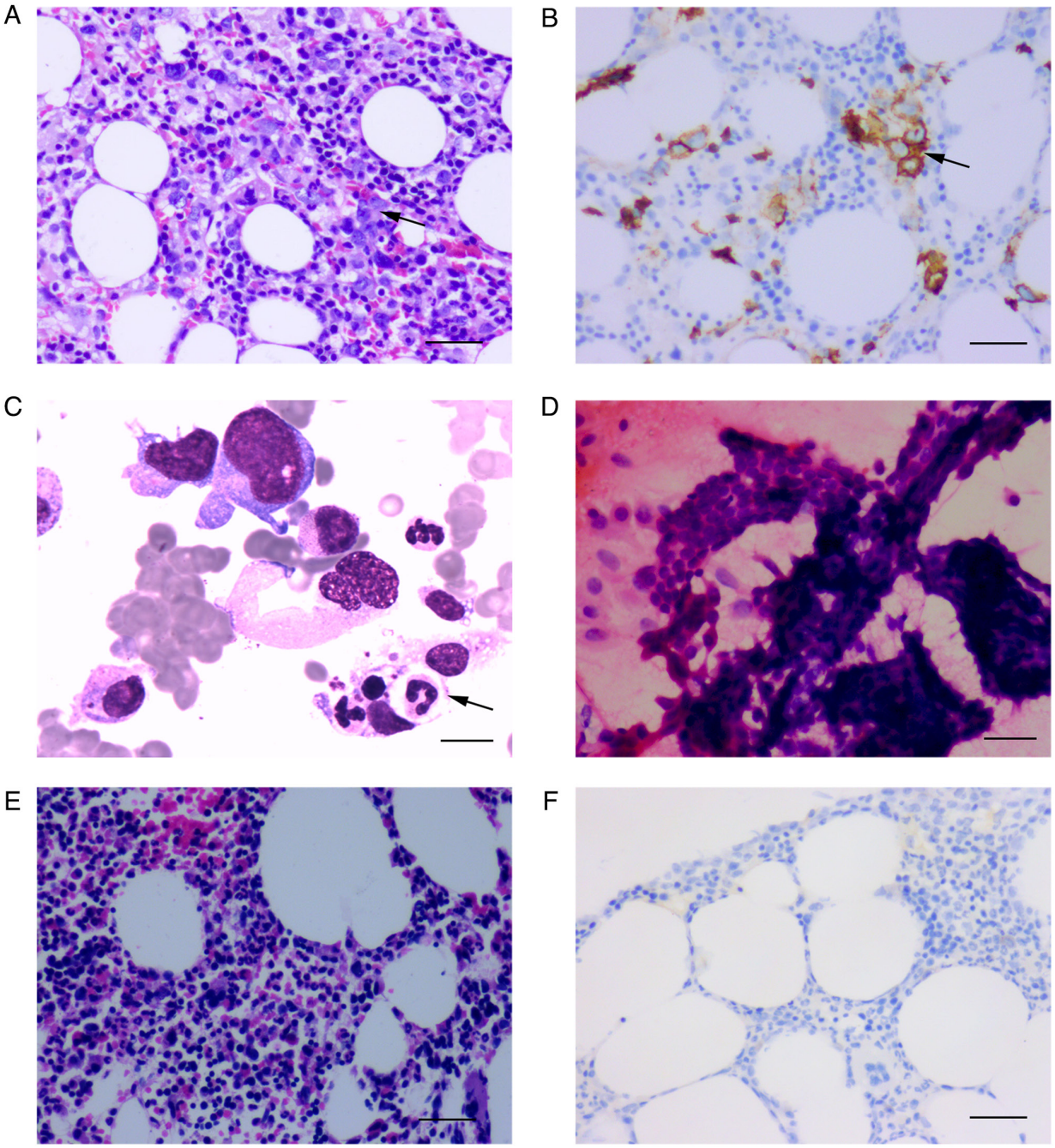

Figure 1. Photomicrographs samples of bone marrow and thyroid. (A) Haematoxylin and eosin sample of bone marrow before treatment (magnification, x200; scale bar, 100 μm). (B) Immunostained sample of bone marrow showing CD20 positive before treatment (magnification, x200; scale bar 100 μm). (C) Photomicrograph sample of bone marrow showing neutrophils engulfed by macrophages (black arrow) (scale bar, 20 μm). (D) Photomicrograph of fine needle aspiration biopsy sample suggesting papillary thyroid carcinoma (magnification, x400; scale bar, 20 μm). (E) Haematoxylin and eosin sample of bone marrow after four cycles of treatment (magnification, x200; scale bar, 100 μm). (F) Immunostained sample of bone marrow showing CD20 negative after four cycles of treatment (magnification, x200, scale bar 100 μm).

calculated as follows: (ng/μl x10^5)/[660 g/mol x average library size (bp)]=Molarity (nM).

Next-generation sequencing analysis. The quality control process Fastp (version 0.23.2; https://github.com/OpenGene/fastp) was applied for FASTQ data by removing the terminal adaptor sequences and low-quality reads from the raw data. Dragen (version 3.10.4; Illumina, Inc.), a local installation hardware-accelerated sequencing processing pipeline, was used to perform data alignment and mutation calling. The lower limit of detection for variant allele frequency was 0.5%, and then an in-house algorithm was used to review hotspot variants. The final candidate variants were all manually verified in the Integrative Genomics Viewer (IGV; https://www.igv.org/). Copy number alterations were identified using CNVkit (version 0.9.10; https://cnvkit.readthedocs.io/en/stable/) with default parameters. The insertion and deletion caller Pindel (version v0.2.5b8; http://gmt.genome.wustl.edu/pack-ages/pindel/) and FLT3_ITD_ext (26) (version 1.1; https://github.com/ht50/FLT3_ITD_ext) were run

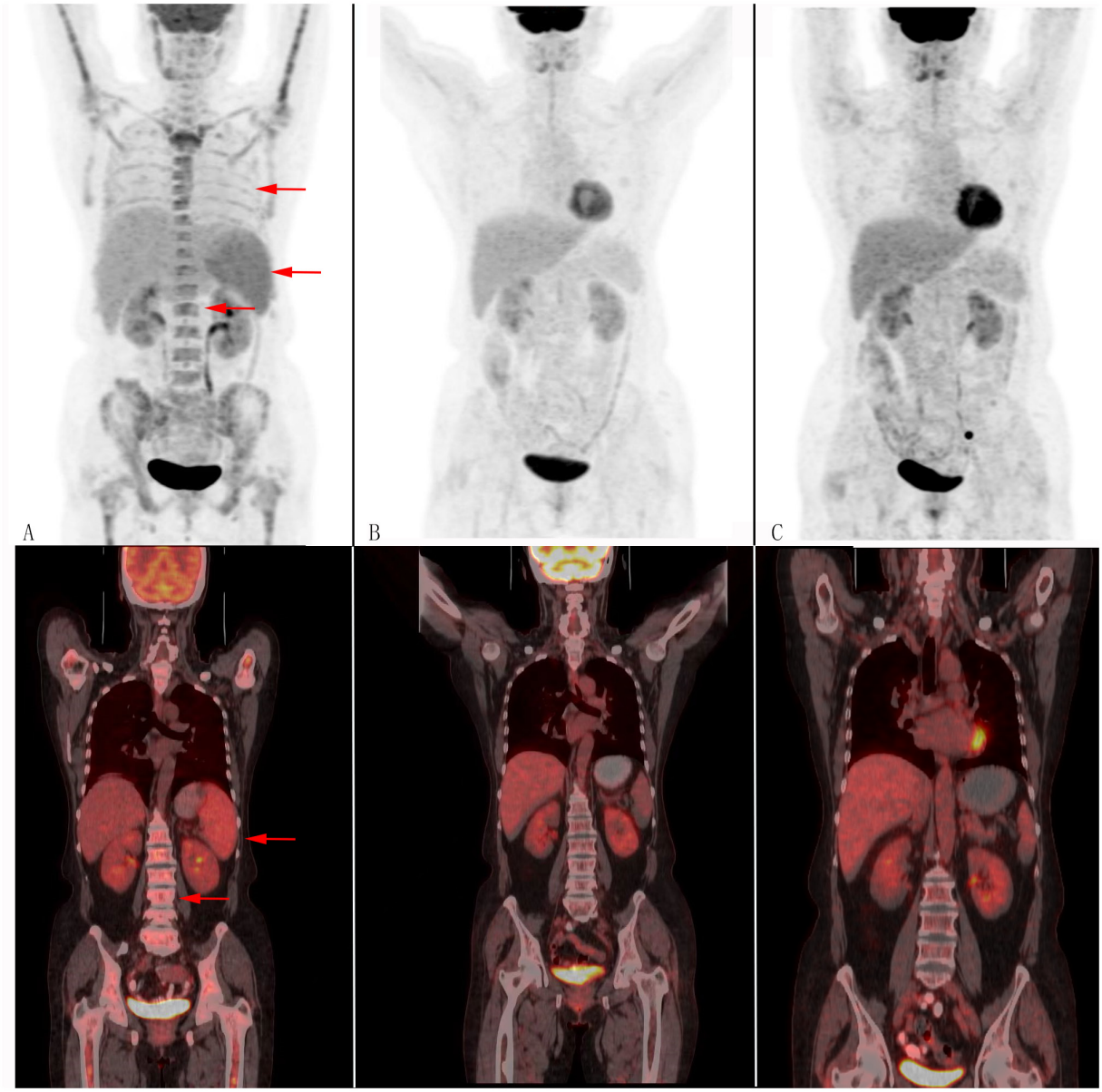

Figure 2. PET/CT finding. (A) PET/CT images showing splenic enlargement and diffuse hypermetabolism (SUVmax=4.6), both lungs (SUVmax=1.5) and bone marrow (SUVmax=1.8-5.9) before treatment (red arrow). (B) The volume and metabolism of the spleen, both lungs and bone marrow are normal after four cycles of treatment. (C) PET/CT images showing metabolism in these organs remaining normal after 8cycles of treatment. PET/CT, positron emission tomography/computed tomography.

on exon 13-15 to identify FMS-like tyrosine kinase 3 internal tandem duplication alleles.

IgH gene monoclonal rearrangement was identified by polymerase chain reaction-based Genescan analysis of bone marrow. Chromosome immunofluorescence *in situ* hybridisation analysis revealed that the *BCL2*, *BCL6* and *MYC* genes had no rearrangement (Fig. S4). A total of 2 ml of bone marrow were drawn and added to a 15-ml centrifuge tube. A total of 5 ml of saline was injected and thoroughly mixed. Then the samples were centrifuged and hypotonic solution was added.

The samples were prefixed and fixed (methanol: glacial acetic acid 3:1) three times successively. After each fixation, the supernatant was centrifuged at 1,800 rpm and discarded. The fixed liquid was composed of methanol and glacial acetic acid at 3:1. The sample concentration was adjusted, the cells dropped on the slide and air dried. Microscopic examination was conducted to find the marks of well-dispersed cells. Then the slides were washed with 2X SSC solution, rinsed with deionized water, dehydrated with gradient ethanol, and then air-dried.

A total of 2 μl probe solution was added to 8x80-mm cover glass and the edge was sealed with film sealant. In the hybridizer, denatured at 88˚C for 2 min and hybridized at 45˚C for >2 h. The sealing glue and cover glass were carefully removed, and washed in 0.3% NP-40/0.4X SSC solution at 73˚C and 0.1% NP-40/2X SSC solution at room temperature. A total of 2 μl DAPI was added to a 12x12-mm cover slide, and the slide with cells was inverted on the cover slide, stored away from light at 20˚C, and finally observed under a fluorescence microscope.

Based on the aforementioned findings, the patient was diagnosed with HPS-associated IVLBCL (Ann Arbor IVB,

Table II. Previously reported cases of IVLBCL involved the thyroid.

First author/s, year	Age	Sex	Diagnosis	Treatment	Outcome	(Refs.)
Stonecypher *et al*, 2014	68	Male	IVLBCL + PTC	Total thyroidectomy + methotrexate + R-CHOP	In favourable condition	(10)
Linnik *et al*, 2018	79	Female	IVLBCL	3 courses of R-CHOP	No recurrence after follow-up	(14)
Saleem *et al*, 2023	70	Female	IVLBCL	Total thyroidectomy	Disease-free after 2 years	(11)
Luo *et al*, 2017	68	Male	IVLBCL	Total thyroidectomy, but declined chemotherapy	Died in the fifth month after operation	(13)
Rea *et al*, 2020	70	Female	IVLBCL	Total thyroidectomy	-	(12)
Teo *et al*, 2022	65	Male	IVLBCL + thyroid mucormycosis	3 courses of R-CHOP + total thyroidectomy	Succumbed to lymphoma relapse 2 years later	(9)
Gaul *et al*, 2006	68	Male	IVL+ autopsy revealed tumor in heart and thyroid	-	Died before a definitive diagnosis	(15)
Darko *et al*, 2006	69	Male	IVLBCL	-	Died because of heart failure	(16)

IVLBCL, intravascular large B-cell lymphoma.

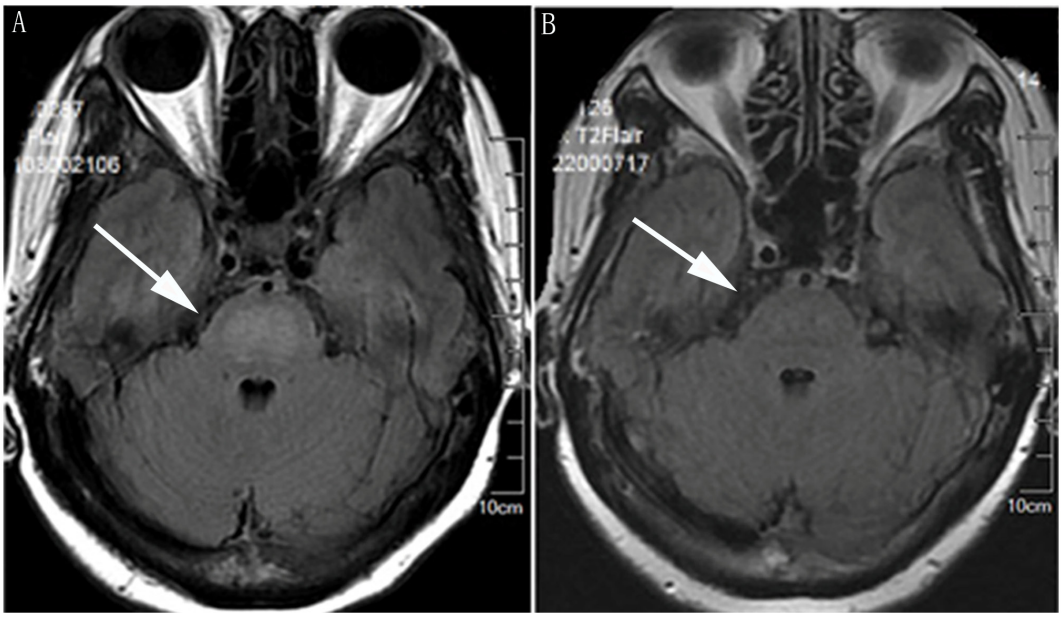

Figure 3. Cranial T2-weighted MRI. (A) MRI showing a hyperintense lesion in the central pons (white arrow) after one cycle of treatment. (B) MRI showing the hyperintense lesion is almost undetectable in the central pons (white arrow) after four cycles of treatment. MRI, magnetic resonance imaging.

IPI 3 scores) and PTC. On the second day of treatment with the HLH-1994 and ruxolitinib treatment protocol, the patient's high fever, which had consistently been present for more than a month, normalised. Tests for EBV were negative after treatment with acyclovir and one course of R-CHOPE therapy comprising rituximab, cyclophosphamide, hydroxydaunorubicin, vincristine, prednisone and etoposide [rituximab 600 mg, intravenous guttae (ivgtt): day 0 (D0); etoposide 0.1 g ivgtt: D1-2; cyclophosphamide 1,000 mg ivgtt: D1; doxorubicin liposomes 40 ms ivgtt: D1; vincristine 2 mg ivgtt: D1; and prednisone 100 mg p.o: D1-5]. After 4 courses of chemotherapy, a bone marrow biopsy showed an absence of tumour cells (Fig. 1). Throughout these 4 courses of treatment, PET/CT images showed complete remission (Fig. 2) and serum

titres of cytokines normalised. The patient refused to consent for treatment of her PTC by thyroidectomy. At the time of submitting this article, the patient had undergone 8 courses of chemotherapy and 4 courses of intrathecal chemotherapy (methotrexate 10 mg) and PET/CT had shown a complete response (Fig. 2). She has been taking zanubrutinib 80 mg orally twice daily for 1.5 years and remains in remission.

Discussion

A literature search revealed 8 previously reported cases of IVLBCL that involved the thyroid (9-16) (Table II). These patients presented with diverse symptoms and had poor prognoses. IVLBCL and PTC occurred concurrently in only 1 of these patients (10). In that patient, IVLBCL was initially diagnosed by PET/CT and subsequently confirmed by bone marrow biopsy. In our patient, fine needle aspiration biopsy of the thyroid revealed only PTC. PET/CT showed thyroid and lung hypermetabolism. The decrease in PET/CT metabolism after chemotherapy suggested that IVLBCL may had invaded the thyroid and lung. It was nto possible to confirm this because the patient did not undergo total thyroidectomy or lung biopsy. It has been reported that, even in the absence of neurological symptoms, ~90% of patients with IVLBCL have abnormalities on pre-treatment brain MRI and that hyperintense lesion in the pons on T2WI are potentially of diagnostic value (17). No brain lesions were definitively diagnosed because brain biopsy is difficult. In our patient, the hyperintense lesion revealed on a pre-treatment MRI had completely resolved by four courses of treatment.

M-protein, usually associated with plasma-cell dyscrasias, is also often reported in other B-cell malignancies, and is reportedly always an independent prognostic marker of poor outcomes (18). However, M-protein is rarely found in patients with IVLBCL. Findings on immunofixation electrophoresis in our patient suggested that the differential diagnosis should have included both multiple myeloma and IVLBCL. Flow cytometric analyses were negative for plasma cell labelling and bone marrow biopsy identified CD20- and PAX-5-positive large cells within vascular spaces, both of which are distinguishing features.

Studies have shown that patients with IVLBCL with double expression have lower rates of complete remission and higher mortality rates than those without double expression (19). It has been found that deficiency of BCL2, which is an anti-apoptotic proto-oncoprotein, is associated with thyroid tumour dedifferentiation (20). Expression of BCL2 is reportedly significantly stronger in patients with PTC than in healthy individuals (21). Differences in effects of BCL2 between IVLBCL and PTC need further research.

In individuals with autoimmune diseases, the incidence of cancers such as non-Hodgkin's lymphoma and thyroid cancer increase (22). Xerophthalmia, antinuclear antibody titre of our patient was 1:1,000 and the titres of various cytokines were higher than normal, prompting consideration of autoimmune diseases, such as Sjogren's syndrome. Sjogren's syndrome American College of Rheumatology/European Alliance of Association for Rheumatology criteria are based on the weighted sum of 5 items: anti-SSA antibody positivity, focal lymphocytic sialadenitis, an abnormal ocular staining score ≥5, a Schirmer test ≤5 mm/5 min and an unstimulated salivary flow rate ≤0.1 ml/min (23), which were not met in our patient.

HLH, triggered by malignancies, consists of uncontrolled activated lymphocytes and macrophages that secrete excessive cytokines (24). The HLH-2004 protocol still forms the basis of the diagnosis of HLH in adults and treatment of HLH is primarily based on the HLH-94 protocol. Our patient was considered for HLH secondary to IVLBCL, met the HLH-2004 and was treated with HLH-94 protocol (8). It has been reported that serum interleukin-10 (IL-10) concentration has a diagnostic sensitivity and specificity for IVLBCL of 80 and 100%, respectively, when the cutoff value is 95.65 pg/ml (25). Our patient's IL-10 concentration decreased to <30 pg/ml. The present findings support the role of serum IL-10 as a valuable biomarker for early diagnosis and monitoring of treatment in patients with IVLBCL.

The pathological mechanism underlying simultaneous IVLBCL and PTC is unknown. Second-generation sequencing in our patient showed a high frequency of *CCND1* mutation. The *CCND1* gene encodes the cyclin D1 oncogene product, a major regulator of G1-S transition in the cell cycle. Aberrant expression of cyclin D1 protein has been implicated in the pathogenesis of several types of human neoplasms (26). Pathological examination of a sample of our patient's marrow revealed aberrant cyclin D1 expression.

DNMT3A encodes an enzyme of DNA methylation. DNA methylation is involved in both lymphomagenesis and progression and relapse of lymphomas (27). Our patient was 63 years old, infected with EBV, and had *DNMT3A* mutations. Clonal haematopoiesis, which is associated with *DNMT3A* mutation, leads to systemic inflammation (28). A previous study regarding the pathological mechanisms underlying PTC found an association between chronic inflammation and risk of developing PTC (29).

In the present study, an interesting case that extends our understanding of the simultaneous presence of HPS-associated IVLBCL and PTC was presented. The mechanisms for this association are complex, possibly including having a high frequency of *CCND1* mutation, or EBV infection, or Sjögren's syndrome. It is therefore feasible that a combination of ruxolitinib and chemotherapy would be an effective treatment for HPS-associated IVLBCL and an autoimmune disease. In conclusion, because our experience is limited to one patient, further research is needed to explore the potential pathogenesis of simultaneous IVLBCL and PTC.

Acknowledgements

Not applicable.

Funding

No funding was received.

Availability of data and materials

The datasets generated in the present study may be found in the National Center for Biotechnology Information database under accession number PRJNA1205904 or at the following URL: https://www.ncbi.nlm.nih.gov/sra/PRJNA1205904.

Authors' contributions

JieL and YL initiated and designed the study. JinL, QW and BL collected data and performed the immunohistochemical staining and histopathology. JinL, JY and JieL drafted the final manuscript. YL and JY critically revised of the manuscript for key intellectual content. All authors read and approved the final version of the manuscript. JinL and YL confirm the authenticity of all the raw data.

Ethics approval and consent to participate

Not applicable.

Patient consent for publication

Consent for the publication of data and associated images was provided by the patient.

Competing interests

The authors declare that they have no competing interests.

References

1. Crilley P: Intravascular large B-cell lymphoma: An elusive disease. Oncol Times 40: 16-17, 2018.
2. Shimada K and Kiyoi H: Current progress and future perspectives of research on intravascular large B-cell lymphoma. Cancer Sci 112: 3953-3961, 2021.
3. Sukswai N, Lyapichev K, Khoury JD and Medeiros LJ: Diffuse large B-cell lymphoma variants: An update. Pathology 52: 53-67, 2020.
4. Liu Y, Ma Y, Zhou H, Zhou X and Shao J: Analysis of clinicopathological features and prognostic factors of non-Hodgkin's intravascular large B-cell lymphoma. Oncol Lett 20: 43, 2020.
5. Shimada K, Yoshida K, Suzuki Y, Iriyama C, Inoue Y, Sanada M, Kataoka K, Yuge M, Takagi Y, Kusumoto S, *et al*: Frequent genetic alterations in immune checkpoint-related genes in intravascular large B-cell lymphoma. Blood 137: 1491-1502, 2021.
6. Geer M, Roberts E, Shango M, Till BG, Smith SD, Abbas H, Hill BT, Kaplan J, Barr PM, Caimi P, *et al*: Multicentre retrospective study of intravascular large B-cell lymphoma treated at academic institutions within the United States. Br J Haematol 186: 255-262, 2019.
7. Shimada K, Yamaguchi M, Atsuta Y, Matsue K, Sato K, Kusumoto S, Nagai H, Takizawa J, Fukuhara N, Nagafuji K, *et al*: Rituximab, cyclophosphamide, doxorubicin, vincristine, and prednisolone combined with high-dose methotrexate plus intrathecal chemotherapy for newly diagnosed intravascular large B-cell lymphoma (PRIMEUR-IVL): A multicentre, single-arm, phase 2 trial. Lancet Oncol 21: 593-602, 2020.
8. Ponnatt TS, Lilley CM and Mirza KM: Hemophagocytic lymphohistiocytosis. Arch Pathol Laboratory Med 146: 507-519, 2022.
9. Teo SCF, Fu EWZ, Bundele MM, Hoe JKM, Ling LM, Lim MY and Gan JYJ: Intravascular large B-cell lymphoma associated with sudden stridor arising from thyroid mucormycosis and concomitant bacterial infection. Ann Acad Med Singap 51: 189-191, 2022.
10. Stonecypher M, Yan Z, Wasik MA and LiVolsi V: Intravascular large B cell lymphoma presenting as a thyroid mass. Endocr Pathol 25: 359-360, 2013.
11. Saleem K, Nasrazadani A, Kuang C, Jaitly V, Ho J, Raptis A, Smith R and Seaman C: Intravascular lymphoma-the creepy crawler: A case series and brief literature review. Cancer Diagn Progn 3: 31-37, 2022.
12. Rea B, Peel RL, Han M, Ohori NP and Aggarwal N: Intravascular large B-cell lymphoma involving multinodular goiter and mimicking carcinoma. Int J Surg Pathol 28: 517-518, 2019.
13. Luo B, Chen JM, Liu J, Li WH, Shi YX, Zeng P, Xie YH and Zhang HF: A case of intravascular large B cell lymphoma presenting as nodular goiter. Diagn Pathol 12: 64, 2017.
14. Linnik Y, Nicka C, Lansigan F, Loo E and Liu X: Intravascular Large B-cell lymphoma within a thyroid nodule: A diagnostic pitfall. Int J Surg Pathol 26: 428-431, 2018.
15. Gaul C, Hanisch F, Neureiter D, Behrmann C, Neundörfer B and Winterholler M: Intravascular lymphomatosis mimicking disseminated encephalomyelitis and encephalomyelopathy. Clin Neurol Neurosurg 108: 486-489, 2006.
16. Katalinić D, Valković T, Lucin K and Rudez J: Intravascular lymphoma and thyroid gland. Coll Antropol 30: 239-241, 2006.
17. Abe Y, Narita K, Kobayashi H, Kitadate A, Takeuchi M, Kikuchi Y, Ouchi T, Takeuchi K and Matsue K: Clinical value of abnormal findings on brain magnetic resonance imaging in patients with intravascular large B-cell lymphoma. Ann Hematol 97: 2345-2352, 2018.
18. Cox MC, Esposito F, Postorino M, Venditti A and Di Napoli A: Serum paraprotein is associated with adverse prognostic factors and outcome, across different subtypes of mature B-cell malignancies-A systematic review. Cancers (Basel) 15: 4440, 2023.
19. Boonsakan P, Iamsumang W, Chantrathammachart P, Chayavichitsilp P, Suchonwanit P and Rutnin S: Prognostic value of concurrent expression of C-MYC and BCL2 in intravascular large B-cell lymphoma: A 10-year retrospective study. Biomed Res Int 2020: 1350820, 2020.
20. Gupta A, Jain S, Khurana N and Kakar AK: Expression of p63 and Bcl-2 in malignant thyroid tumors and their correlation with other diagnostic immunocytochemical markers. J Clin Diagn Res 10: EC04-EC08, 2016.
21. Zhang C, Bo C, Guo L, Yu P, Miao S and Gu X: BCL2 and hsa-miR-181a-5p are potential biomarkers associated with papillary thyroid cancer based on bioinformatics analysis. World J Surg Oncol 17: 221, 2019.
22. Zhou Z, Liu H, Yang Y, Zhou J, Zhao L, Chen H, Fei Y, Zhang W, Li M, Zhao Y, *et al*: The five major autoimmune diseases increase the risk of cancer: Epidemiological data from a large-scale cohort study in China. Cancer Commun (Lond) 42: 435-446, 2022.
23. Shiboski CH, Shiboski SC, Seror R, Criswell LA, Labetoulle M, Lietman TM, Rasmussen A, Scofield H, Vitali C, Bowman SJ, *et al*: 2016 American College of Rheumatology/European League against rheumatism classification criteria for primary Sjögren's syndrome: A consensus and data-driven methodology involving three international patient cohorts. Arthritis Rheumatol 69: 35-45, 2016.
24. Kaçar AG and Celkan TT: Hemophagocytic Lymphohistiocytosis. Balkan Med J 39: 309-317, 2022.
25. Zhang Y, Wang L, Sun J, Wang W, Wei C, Zhou D and Zhang W: Serum interleukin-10 as a valuable biomarker for early diagnosis and therapeutic monitoring in intravascular large B-cell lymphoma. Clin Transl Med 10: e131, 2020.
26. Vela-ChÁvez T, Adam P, Kremer M, Bink K, Bacon CM, Menon G, Ferry JA, Fend F, Jaffe ES and Quintanilla-Martínez L: Cyclin D1 positive diffuse large B-cell lymphoma is a post-germinal center-type lymphoma without alterations in theCCND1gene locus. Leuk Lymphoma 52: 458-466, 2011.
27. Vanessa S, Caroline B, Alboukadel K, Devin J, Cartron G, Costes-Martineau V and Moreaux J: An epigenetic regulator-related score (EpiScore) predicts survival in patients with diffuse large B cell lymphoma and identifies patients who may benefit from epigenetic therapy. Oncotarget 9: 19079-19099, 2018.
28. Venanzi A, Marra A, Schiavoni G, Milner SG, Limongello R, Santi A, Pettirossi V, Ultimo S, Tasselli L, Pucciarini A, *et al*: Dissecting clonal hematopoiesis in tissues of patients with classic hodgkin lymphoma. Blood Cancer Discov 2: 216-225, 2021.
29. Pagano L, Mele C, Sama MT, Zavattaro M, Caputo M, De Marchi L, Paggi S, Prodam F, Aimaretti G and Marzullo P: Thyroid cancer phenotypes in relation to inflammation and autoimmunity. Front Biosci (Landmark Ed) 23: 2267-2282, 2018.